Performance Enhancement of Bio-fouling Resistant Cellulose triacetate-based Osmosis Membranes using Functionalized Multiwalled Carbon Nanotube & Graphene Oxide

A.K. GHOSH[1], RUTUJA S. BHOJE[2] AND R.C. BINDAL[1]

[1]Membrane Development Section, Chemical Engineering Group, Bhabha Atomic Research Centre, Trombay, Mumbai – 400 085, India.

[2]Department of Chemical Engineering, Institute of Chemical Technology, Nathalal Parekh Marg, Matunga, Mumbai - 400019, India.

ABSTRACT

In this study, cellulose triacetate (CTA) based nanocomposite membranes were developed by incorporation of carboxylic acid functionalized multiwalled carbon-nanotube (cMWCNT) and graphene oxide (GO) which have enhancement of both flux and fouling resistance properties of the membranes. Membranes were casted at room temperature and annealed at 90°C hot water for 10 minutes. The incorporation level of both the nanomaterials is 1.5% of the CTA polymer weight in the nanocomposite membranes. Prepared membranes were characterized in terms of water contact angle, surface morphology and mechanical strength. The performance of the membranes was evaluated both in reverse osmosis (RO) and forward osmosis (FO) mode. The water flux is observed to increase by ~43% in CTA-cMWCNT and ~69% in CTA-GO membranes than the pure CTA membranes in RO mode (2000ppm NaCl feed at 1551kPa applied pressure) but it is ~41% and ~86% in FO mode (DI water as feed & 1.0 molar NaCl as draw solution) for CTA-cMWCNT and CTA-GO membranes respectively. Nanocomposite membranes containing functionalized CNT & GO were found more biofouling resistant property. The flux recovery is ~62% in pure CTA membrane, whereas it is ~73% for CTA-cMWCNT and ~82% for CTA-GO membranes.

Keywords: Membrane, Osmosis, Cellulose triacetate, Functionalized carbon nanotube, Graphene oxide.

J. Polym. Mater. Vol. **37,** No. 1-2, 2020, 109-120

Correspondence author e-mail: akghosh@barc.gov.in
DOI : https://doi.org/10.32381/JPM.2020.37.1-2.8

INTRODUCTION

Reverse osmosis (RO) is a well-known commercially successful membrane process works on the driving force generated from applied external pressure excess to osmotic pressure of feed. Forward osmosis (FO) based on natural phenomenon of osmosis is found as a novel membrane process used nowadays as a sustainable alternative to reverse osmosis (RO) in many applications [1,2]. In the FO process, the water flows from the solution with lower osmosis pressure to that of higher osmosis pressure (called "draw" solution) across the designed semi-permeable membrane without any external energy consumption [3]. Only osmotic pressure is the driving force for mass transport in FO and hence it possesses advantages of high energy efficiency, low fouling tendency, simplicity in operation compared to RO [4, 5]. The FO process has been successfully applied in several fields like desalination of brackish and sea water [6-9], wastewater treatment [10, 11], concentration of pharmaceuticals [12], concentration of fruit juices and liquid food processing [13-15]. Recently, FO has been successfully used in treatment of radioactive effluents [16-18]. Most of the commercial FO membranes are based on cellulosic & polyamide polymer. Even though the performance of cellulosic membranes is better than polyamide in FO process due to its more hydrophilic nature, the cellulosic membranes are prone to biofouling. However, cellulose triacetate (CTA) membranes have been successfully used for wastewater with severe biofouling due to its good chlorine resistance [19]. To increase permeability and selectivity alongwith better fouling resistance, a new class of membranes was designed by combining polymeric materials with nanomaterials which are known as mixed-matrix nanocomposite membranes [20]. Several nanomaterials that show the maximum promise so far are carbon nanotubes (CNTs), metal and metal oxides, graphene and graphene oxide (GO), and zwitter-ionic materials [21,22]. However, as CNT and GO are carbon-based nanomaterials, they have extra advantage of better compatibility with organic polymers than the inorganic nanomaterials like metal and metal oxides. CNTs were used widely to make nanocomposite membrane for water purification due to its excellent mechanical, thermal, electrical and chemical properties alongwith very high aspect ratio and fast water transport [23-25]. In addition, hydrophilic functional groups like amine or carboxylic acid functionalized CNTs are more useful to make the membrane more hydrophilic and increase the water permeability. Similarly, a graphene derivative, GO is another carbon nanomaterial having high specific surface area with excellent electrical, thermal, optical and mechanical properties and its composite with polymers can very effectively enhance the performance of the nanocomposite membranes even at a very low loading [26, 27]. In addition, GO based membranes also show chlorine resistance and anti-fouling properties [28-30].

This paper presents development of performance enhanced and bio-fouling resistant osmosis membrane by embedding two selected nanomaterials namely, carboxylated multiwalled carbon nanotube and graphene oxide into the cellulose triacetate membrane matrix. The effects of nanomaterials on physico-chemical properties and filtration performance of CTA based composite osmosis membranes have been evaluated.

EXPERIMENTAL

Materials

Cellulose triacetate (CTA) (Mn=72000-74000 Da) polymer was procured from M/s.Sigma-Aldrich, India. Solvents like 1,4-Dioxane, acetone and methanol (all laboratory reagent grade) were obtained locally and used without any further purification. Maleic acid and sodium chloride salt were of analytical grade and procured locally. Carbon nanotube (multi-walled), carboxylic acid functionalized (>8% carboxylic acid functionalized, avg. dia. × L : 9.5 nm × 1.5 µm) and graphene oxide (powder, 15-20 sheets, 4-10% edge-oxidized, Bulk Density: ~1.8 g/cm3) were procured from M/s. Merck, India.

Casting Solution Preparation

In an airtight glass bottle, 13 g of dried moisture free cellulose triacetate (CTA) polymer was added into 58.8 g of 1,4-Dioxane and 19.7 g of acetone solvent mixture and the solution was kept agitated for several hours for complete dissolution. 4.9 g of maleic acid and 3.6 g methanol were subsequently added and the mixture solution was homogenized.

Preparation of osmosis membranes

FO membranes were prepared by commonly used phase inversion technique. The viscous polymer solution was spread over a nonwoven fabric support (Viledon grade H1006 obtained from M/S. Freudenberg Nonwovens India Pvt. Ltd.) with thickness of ~100 µm using doctor knife edge under a steady casting shear. The gap between the fabric and knife-edge (casting thickness) was maintained at 125-130 µm. It was then kept in air for 30 seconds for evaporation of volatile solvents viz. acetone and methanol followed by immersion in a gelling bath containing ultra-pure water at room temperature. After providing sufficient time (~30-35 minutes) to complete the leaching of solvent and additives from the membrane matrices, the resulting membranes were taken out of the gelling water bath and rinsed in fresh water for several times. The gelled membranes are subsequently annealed at 90°C hot water for 10 minutes to get pore shrinked membranes suitable for osmosis applications. The final membrane thickness of all the membranes were found almost same and it is in the range of 160-165 µm (i.e. ~60-65 µm over the fabric). The entire process was carried out in a controlled environmental atmosphere with relative humidity~ 35-40% and temperature of 25°C.

Characterizations of the osmosis membranes

The surface roughness of all the membrane surfaces were carried out by using an Atomic Force Microscope (AFM) instrument (Make: NT-MDT, Model: SOLVER next, Ireland). As membrane samples are soft, semi-contact or tapping mode was used. The cantilever of nominal tip apex radius of 10 nm with a spring constant of 11.8 N/m and having a typical resonance frequency of 240 kHz was used. The scanning was done onto 5 nm × 5 nm area of each membrane with a scanning frequency of 0.3 Hz. The roughness parameters of the membranes are quantitatively reported in terms of average roughness (Ra).

The surface homogeneity of the membranes was characterized using scanning electron microscopic (SEM) images. At first the membrane samples were made electrically conductive by coating the surface with gold-palladium using sputter coater. Then micrographs were recorded using SEM machine (Model:CamScan 3200LV) with acceleration voltage of 10 keV and 10000X magnifications. To get an idea about the hydrophilicity of the membranes, static water contact angle measurements at ambient temperature were conducted using sessile drop method and a contact angle measuring instrument (DSA 100 of KRUSS GmBH, Germany) was employed. At least five measurements maintaining same residence time and drop size were done at different locations of each membrane coupons and taken the average value of contact angle. Mechanical strength of all the membranes was characterized by the ultimate tensile strength measured using a mechanical testing instrument (Instron 5540 Series Single Column Testing Systems; Instron, Norwood, Massachusetts, USA). A membrane specimen (5.0 cm×2.0 cm) was stretched at a predetermined rate (0.7 mm/min) until breakage.

RO & FO membrane performance evaluation and biofouling studies

To get the quick idea on whether the prepared membranes are suitable for osmosis applications, all the membranes were characterized in terms of product permeability or flux & salt rejection under standard brackish water RO (BWRO) testing condition (2000 ppm NaCl feed at 1551 kPa pressure). The feed water was pumped across a membrane of area 14.5cm^2 using a reciprocating pump. The schematic details of the experimental set up and the test cell were given in our previous paper [31]. The steady-state flux is calculated by taking the average of three readings taken at a regular time interval. The permeability values obtained as milli Litre/minute (mL/min.) were reported as L.m^{-2}.h^{-1}(LMH). The solute separation data were collected using 2000ppm NaCl feed. Concentration of feed and product was measured by measuring the specific conductance and calculate from the specific conductance vs. concentration calibration plot for NaCl solutions. All the FO experiments were carried out in AL-FS mode (active layer facing feed solution) where the feed was allowed to flow through one side of the membrane while the draw solution was kept flowing across the other side. The photographs of the experimental set up along with the test cells were given in Fig.1. In this system, two gear pumps circulating the draw solution (DS) and the feed solution (FS) on the two sides of the membrane at a crossflow velocity of 20 cm/s. The volume reduced from feed side or volume increase in draw solution side is defined as flux in FO testing. For this experiment, DI water was used as feed and varying concentration [(0.5 (M), 1 (M) and 2 (M)] of NaCl solutions used as draw solutions & flux was calculated by taking average of three readings taken for three different membrane coupons prepared independently. Back diffusion of salt from higher concentration draw solution to the feed side was calculated by mass balance.

For testing of the bacterial retention of the membranes, overnight culture of *E. coli* strain MD 1655 was grown (~8 cfu/L) in sterile Luria broth upon incubation at 37°C under shaking conditions (150 rpm). The bacterial culture thus obtained was used for microbial decontamination and biofouling studies. Sterile saline with bacteria density 8*107 cfu/L was taken and small parts of membrane punches (circular pieces) were dipped in the culture for one hour and direct images were taken to get the idea of bacterial growth over the membrane.

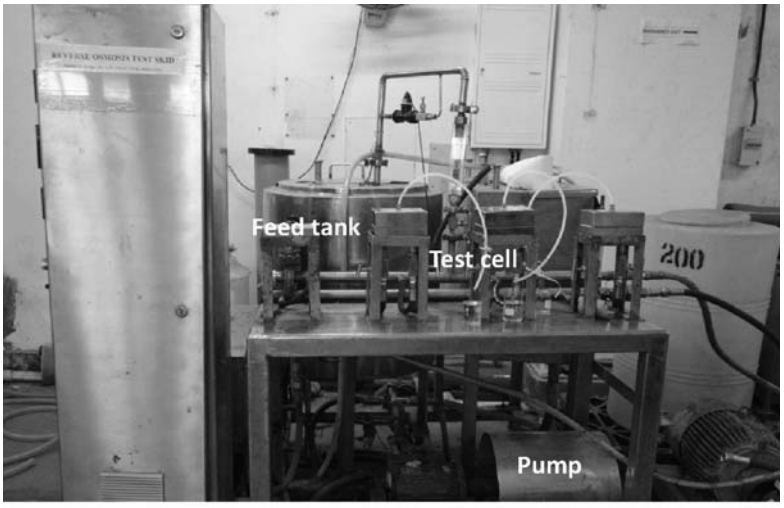

Photograph of RO Test set-up

The fouling experiment was conducted using initial feed and draw solution volumes of 2.5 liters. Then the FO system was operated for 10hrs. (600 minutes) at a crossflow velocity of 9.0 cm/s. *E. coli* bacteria at a concentration of about 107 cfu/L was added to the feed solution to accelerate biofouling which is significantly higher than those encountered in typical operation [32]. Permeate flux decline was continuously monitored using an electronic balance to get an idea of biofouling by both pure polymer and nanocomposite membranes. After this testing, all the membranes were washed with DI water and again tested in FO set up to determine flux recovery after biofouling experiment.

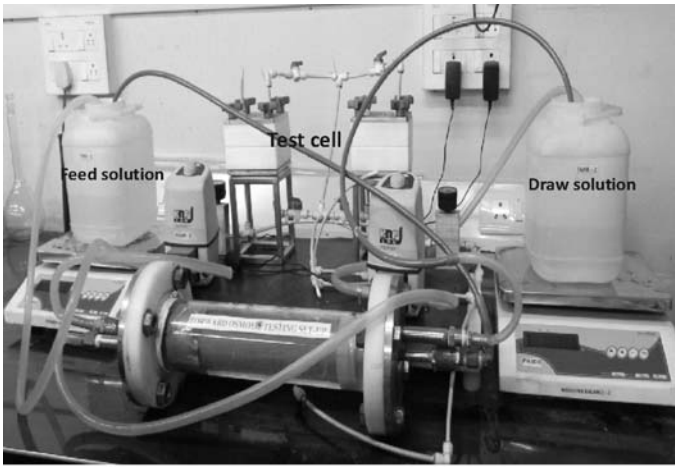

Photographs of FO Test set-up

Fig. 1. Photographs of the RO and FO testing set-up used.

RESULTS AND DISCUSSION

As per the published HTI patent [33], pure CTA membranes were prepared using casting solution composition of CTA-13.1%; 1,4 Dioxane- 52.5%; Acetone -19.7%; Methanol-8.2%, Lactic acid-6.6%. The composition of casting solution was readjusted little bit in the present study with incorporation of new additive and adding maleic acid in place of lactic acid. Here, the details on effect of nanomaterials addition with optimum CTA polymer composition have been studied and reported.

Membrane surface characteristics

The CTA based osmosis membranes prepared with and without nanoparticles were characterized in terms of their water contact angle, surface average roughness and mechanical strength data. Performance of the membranes was evaluated under standard BWRO & FO conditions. The results are given in Table 1. Incorporation of hydrophilic nanomaterials onto CTA membranes exhibits noticeable decrease in water contact angle values because of the inherent hydrophilic nature of both carboxylated-MWCNT & GO nanoparticles owing to their chemical structure which makes the nanocomposite membranes more hydrophilic. GO is found more effective to increase the hydrophilicity than that of carboxylated-MWCNT with same loading of nanomaterials in the polymer matrix. As

leaching of the nanomaterials was not seen in the gelling medium during the membrane preparation, it can be assumed that the loading of both carboxylated-MWCNT & GO is 1.5% of the CTA polymer weight in the nanocomposite membranes. But still the difference in hydrophilicity in carboxylated-MWCNT based membrane with GO based membrane could be due to presence of more carboxylic acid (-COOH) functional group present in GO.

The topography of the membranes top surfaces was investigated through AFM and it is quantified in terms of a roughness parameter *i.e.* average roughness (Ra). With impregnation of nanomaterials, the nanocomposite membrane surfaces are rougher in compare to relatively smooth surface of CTA membranes and the results reflected in the surface average roughness value for the membranes. It also indicates that the nanoparticles are not leaching out in gelling process during membrane preparation. The surface of GO embedded nanocomposite membranes is relatively smoother than the carboxylated-MWCNT based nanocomposite membrane.

Both AFM and SEM images of the membranes are given in Fig.2. The surface morphology of CTA membranes looks quite uniform, but it can be noticed that small agglomeration of nanoparticles were seen in both the nanocomposite membranes. The ultimate tensile strength (UTS) can be used as a measure of the strength of the membrane. As these membranes are casted over non-woven polyester fabric, the UTS of only fabric is also measured and reported. Both tensile strength & percentage elongation at break of the pure polymeric CTA membrane is the lowest and CTA-GO nanocomposite membrane is the highest. The increase of strength of the nanocomposite membranes are indications of proper compatibility of cMWCNT and GO nanomaterials with the CTA polymer and their dispersion ability in casting solution. The presence of functional group like carboxylic acid (-COOH) in both cMWCNT and GO can chemically interact with hydroxyl group (-OH) of CTA to give stable casting solution.

TABLE 1: Properties of the Membranes

Membrane	Water contact angle (o)	Ave. surface roughness (nm)	Ultimate tensile strength (MPa)	Elongation at break (%)
CTA-blank	47.5±0.5	6.30±0.89	23.4±0.6	14.6±0.6
CTA- cMWCNT	42.4±0.9	12.28±1.64	35.5±1.1	16.3±0.9
CTA-GO	39.5±0.8	8.02±1.08	36.9±0.9	17.7±0.6

*Ultimate tensile strength of nonwoven fabric=15.5±0.5 MPa.

Water permeation and salt rejection performance of the membranes

Table 2 represents the performances of nanocomposite membranes alongwith the blank in both reverse osmosis (RO) and forward osmosis (FO) modes. Permeate flux and salt rejection data in BWRO testing were collected when it became constant over 60 minutes. The permeate flux through the membrane in BWRO mode follows the order: blank-CTA<CTA-

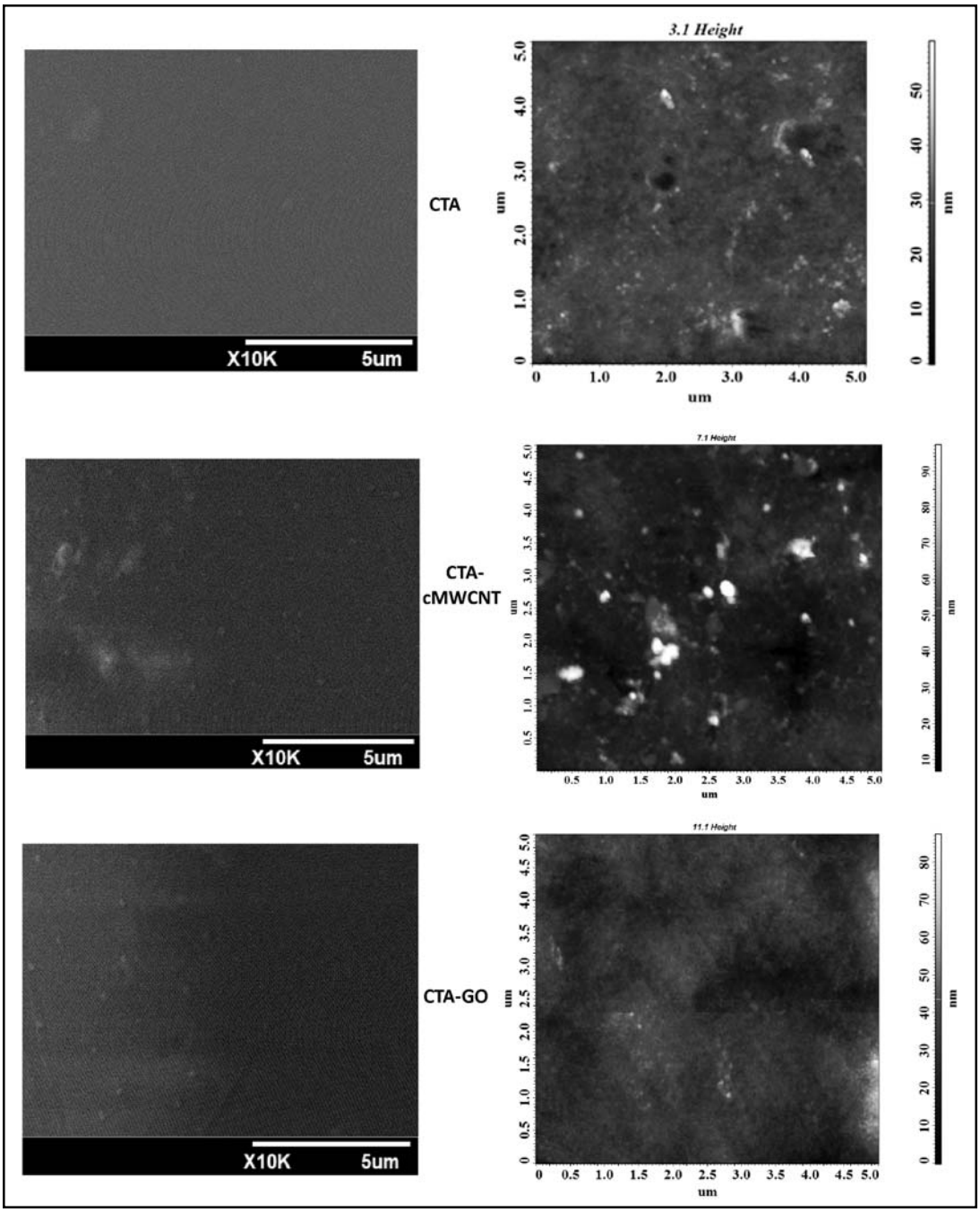

Fig. 2. SEM & AFM images of pure polymer and nanocomposite membranes.

cMWCNT<CTA-GO with almost same salt rejection properties. In FO mode also, water permeation through the membrane follows the same trend as RO and with no change in back diffusion of salt.

The flux increase is observed as ~43% in CTA-cMWCNT and ~69% in CTA-GO membranes in RO mode whereas, the increase in water permeation is observed as ~41% in CTA-cMWCNT and ~86% in CTA-GO membranes in FO mode.

The porous structure of cMWCNT and GO can provide extra channels for permeation of water during the filtration process. The more hydrophilic character as evident from lower water contact angles and rougher surface (to provide more exposed surface area) as evident from AFM roughness values of the nanocomposite membranes are contributed additionally towards more water flux than pure polymer membrane. Preparation of RO membranes in asymmetric form has advantages like it is formed in one step unlike two-step process for TFC membranes but the flux of commercial TFC membrane is more in RO mode. However, performances of the membranes in FO mode are quite encouraging and hence in subsequent section mostly experiments are focused on FO mode testing.

TABLE 2: Membrane RO and FO performance

Membrane	RO performance		FO performance	
	Flux (LMH)	Salt rejection (%)	Flux (LMH)	Back diffusion of salt (%)
CTA-blank	20.4±0.9	94.5±0.8	7.8±0.3	0.53±0.05
CTA- cMWCNT	29.2±1.1	93.8±1.0	11.0±0.3	0.64±0.06
CTA-GO	34.5±1.0	94.0±0.7	14.5±0.4	0.49±0.05

* RO testing: Feed-2000 ppm NaCl, Applied pressure-1551 kPa

* FO testing: Feed-DI water, Draw solution: 1molar NaCl

Membrane performance as a function of concentration of draw solution in FO

The performance of the osmosis membranes in terms of water permeation flux and back diffusion of salt were evaluated in FO mode using DI water as feed and NaCl draw solution of three different concentration [0.5 (M), 1 (M) and 2 (M)]. To minimize the effect of concentration polarization, both feed and draw solutions were circulated across the membrane in AL-FS mode (active layer facing the feed solution). The average value of performance parameters was determined after 5 hours of run and the results are given in Table 3. The percentage increase of water flux on changing draw solution concentration from 0.5–1.0 (M) and from 1.0 - 2.0 (M) is given in Fig. 3 for easy understanding. It was found that both the nanocomposite membranes gave higher water flux with almost same salt back diffusion than the pure CTA membranes at all concentration of draw solutions. CTA-GO membranes have shown the highest water flux with very nominal (upto 0.69%) back diffusion of salt from draw solution to feed. Both water flux and back diffusion of salt increases with

increase of draw solution concentration of all the membranes. However, % of back diffusion of salt for highest concentration draw solution was still very nominal (0.69% to 0.80%) and manageable for practical applications. As the concentration of draw solution increases, osmotic pressure difference between the feed and draw solution increases, resulting in higher driving force for water flow to take place in the FO process. Increase of water flux on increase of draw solution concentration from 0.5-1.0 (M) is distinctly less for CTA membrane (~50%) than that of both the nanocomposite membranes (~59.4% & 61.1%). However, the increase of water flux on increase of draw solution concentration from 1.0-2.0 (M) for CTA membrane (~65.4%) is close to that of both the nanocomposite membranes (~66.4% & 69.7%).

Table 3: Performance of FO membranes as a function of concentration of draw solution

Membrane	Concentration of NaCl in draw solution (M)					
	0.5		1.0		2.0	
	Flux (LMH)	% back diffusion of salt	Flux (LMH)	%back Flux diffusion of salt	Flux (LMH)	%back diffusion of salt
CTA	5.2±0.2	0.24±0.02	7.8±0.3	0.53±0.05	12.9±0.5	0.75±0.08
CTA-cMWCNT	6.9±0.2	0.25±0.03	11.0±0.3	0.59±0.06	18.3±0.7	0.80±0.10
CTA-GO	9.0±0.3	0.21±0.02	14.5±0.4	0.50±0.05	24.6±0.6	0.69±0.09

Feed: DI water

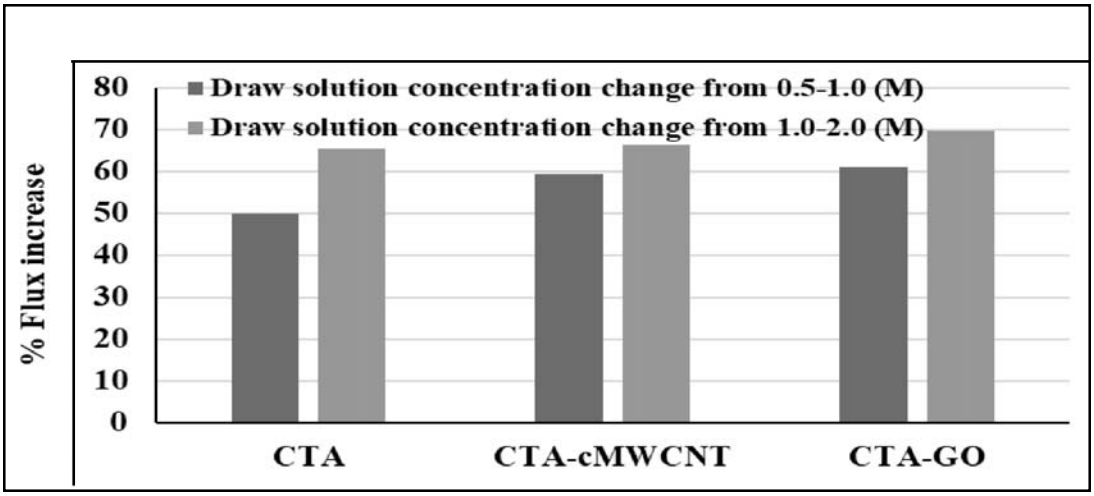

Fig. 3. Percentage water flux increase on increase of draw solution concentration.

Biofouling studies of the membranes

Bio-fouling tests were conducted using E. coli as model biofoulant. Before addition of the bacteria, the water flux was allowed to stabilize at 12.0±0.5 LMH using the adjustment of concentration of draw solution. Obviously, the draw solution concentration for CTA, CTA-cMWCNT and CTA-GO membranes were ~1.8 (M), ~1.2 (M) and 0.8(M) respectively. Here the DI water stabilized flux is taken as J_0 at time zero and then E. coli bacteria solution was added in the feed side and the water flux at time t is denoted as J_w. The plot of normalized flux (J_w/J_0) as a function of time is given in Fig.4. On addition of biofoulants (E. coli) in the feed solution, the water flux started decreasing with time for all the membranes, but nanocomposite membranes exhibit relatively lower flux decline. It is due to the deposition and biofilm formation over the membrane surface. Nanocomposite membranes offered more hydrophilic surface which can result thicker water layer over the membrane and resist bio-foulant deposition some extent on the membrane surface. The lowest flux decline in CTA-GO membrane can be attributed to the presence GO which has anti-microbial property. After this biofouling experiment till 600 minutes., all the membranes were washed with DI water and tested again in FO set up to determine flux recovery. The results of flux recovery experiments are given in Fig.5. The flux recovery in pure polymeric CTA membrane is much less (~62%) than both CTA-cMWCNT (~73%) and CTA-GO (~82%) membranes. This clearly indicates that the bio-film adhesion tendency on pure polymeric membrane is much more than the cMWCNT and GO based nanocomposite membranes.

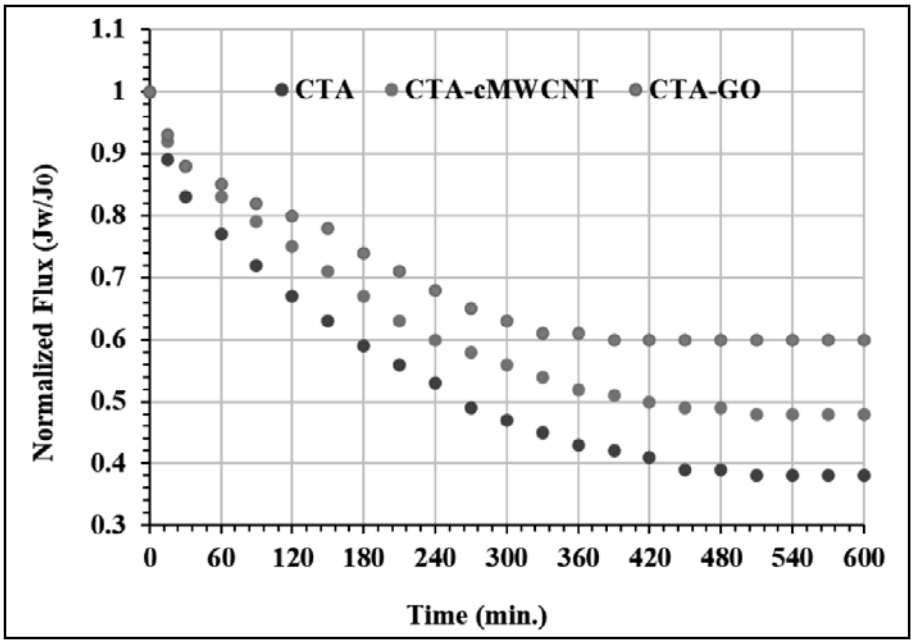

Fig. 4. Flux versus time of FO membranes during E-coli filtration.

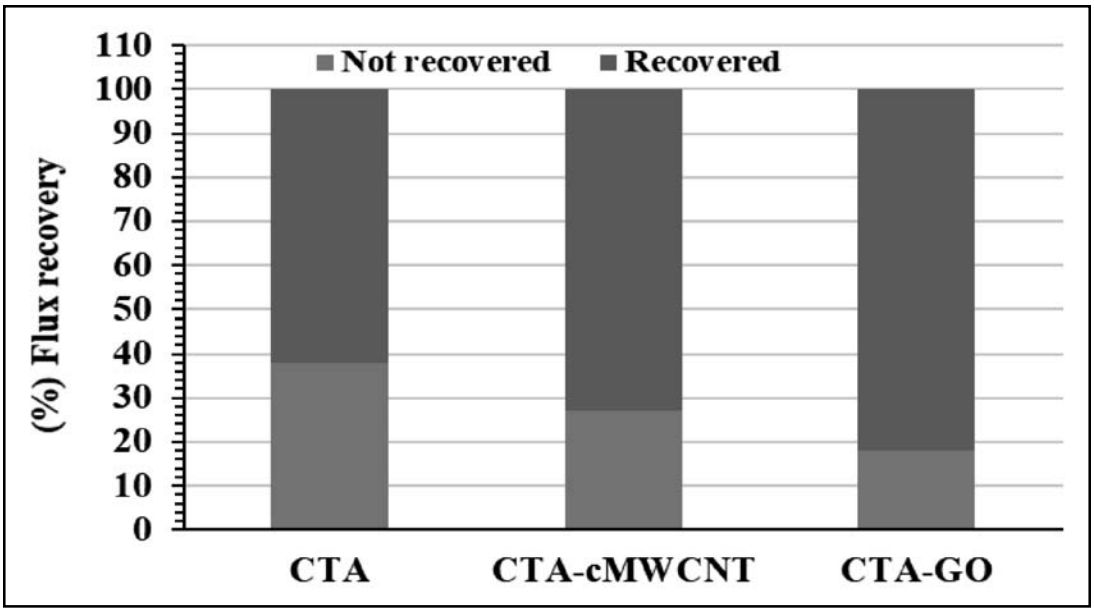

Fig. 5. Flux recovery on washing of FO membranes after biofouling.

CONCLUSIONS

Carboxylated multiwalled carbon nanotube and graphene oxide are two potential nanomaterials for enhancement of performance in terms of water permeation rate with salt rejection and also the mechanical strength which makes nanocomposite membranes of CTA more promising for use in pressure driven membrane application. The performance of the membranes in terms of permeate flux (both in RO & FO mode) is in the order: blank-CTA<CTA-cMWCNT<CTA-GO with almost no change in salt passage properties. The increase of water flux is found as ~43% in CTA-cMWCNT and ~69% in CTA-GO membranes as compared to the pure CTA membranes in RO mode. However, it is ~41% and ~86% for CTA-cMWCNT and CTA-GO membranes respectively in FO mode.

The values of water flux and salt rejection/back diffusion of salts indicate that nanocomposite membranes are typically moderate brackish water reverse osmosis (BWRO) membrane but excellent FO membranes. The FO membrane prepared in the present study can be used with NaCl draw solution as high as 2(M) concentration as the back diffusion of NaCl by the membranes is only 0.7-0.8%. Nanocomposite membranes containing functionalized CNT & GO were found more biofouling resistant than the pure polymer membranes. After flushing with deionized water, the flux recovery in pure CTA membrane is ~62% but is ~73% & ~82% in CTA-cMWCNT and CTA-GO membranes respectively.

REFERENCES

1. M.A. Shannon, P.W. Bohn, M. Elimelech, J.G. Georgiadis, B.J. Marinas, A.M. Mayes, *Nature*, 452 (2008) 301-310.

2. A. Altaee, G. Zaragoza, H. R. Tonningen, *Desalination*, 336 (2014) 50-57.
3. T.Y. Cath, A.E. Childress, M. Elimelech, *J. Membr. Sci.* 281 (2006) 70-87.
4. S. Lee, C. Boo, M. Elimelech, S. Hong, *J. Membr. Sci.*, 365 (2010) 34-39.
5. R.L. McGinnis, M. Elimelech, *Desalination*, 207 (2007) 370-382.
6. S. Zhao, L. Zou, D. Mulcahy, *Desalination*, 284 (2012) 175-181.
7. S. Phuntsho, S. Hong, M. Elimelech, H.K. Shon, *J. Membr. Sci.*, 436 (2013) 1-15.
8. J.R. McCutcheon, R.L. McGinnis, M. Elimelech, *J. Membr. Sci.*, 278 (2006) 114-123.
9. S. Low, *Desal. Water Treat.* 7 (2009) 41-46.
10. A. Achilli, T.Y. Cath, E.A. Marchand, A.E. Childress, *Desalination*, 239 (2009) 10-21.
11. R.W. Holloway, A.E. Childress, K.E. Dennett, T.Y. Cath, *Water research*, 41 (2007) 4005-4014.
12. C.A. Nayak, N.K. Rastogi, *Desal. Water Treat.*, 16 (2010) 134-145.
13. K.B. Petrotos, P. Quantick, H. Petropakis, *J. Membr. Sci.*, 150 (1998)99-110.
14. E. Beaudry, K. Lampi, *Food Technology*, 44 (1990) 121.
15. K.B. Petrotos, H.N. Lazarides, *J. Food Engg*., 49 (2001) 201-206.
16. A.K.Ghosh, R.C.Bindal, S. Prabhakar, P. Tewari, Desal. Water Treat., 52 (2014) 432-437.
17. S. Lee, Y. Kim, J. Park, H.K. Shon, S. Hong, *J. Membr. Sci.* 556 (2018) 238-247.
18. X. Liu, J. Wu, J. Wang, *Chem. Eng. Journal*, 344 (2018) 353-362.
19. G. Kang, Y. Cao, *Water Res.* 46 (3) (2012) 584-600.
20. Y. Wen, J. Yuan, X. Ma, S. Wang, Y. Liu, *Environ. Chem. Letters*, 17 (2019)1539-1551.
21. M.Bassyouni, M.Abdel-Aziz, M. Zoromba, S.Abdel-Hamid, E. Drioli, *J. Indus. Eng. Chem*, 73 (2019) 19-46.
22. R.S. Hebbar, A.M. Isloor, Inamuddin, A.M. Asiri, *Environ. Chem. Lett.* 15 (2017) 643-671.
23. Ihsanullah, *Sep. Purif. Technol.* 209 (2019) 307-337.
24. C. Rizzuto, G. Pugliese, M.A. Bahattab, S.A. Aljlil, E. Drioli, E. Tocci, *Sep. Purif. Technol.* 193 (2018) 378-385
25. K.-J. Lee, H.-D. Park, *J. Memb. Sci.* 501 (2016)144-151
26. M. Hu, B. Mi, *Environ. Sci. Technol.* 47 (8) (2013) 3715-3723.
27. H. Wang, T. Yan, P. Liu, *J. Mater. Chem. A* 4 (13) (2016) 4908-4919.
28. S. Zinadini, A.A. Zinatizadeh, M. Rahimi, *J. Membr. Sci.* 453 (2014) 292-301.
29. J. Lee, H.R. Chae, Y.J. Won, *J. Membr. Sci.* 448 (2013) 223-230.
30. H.R. Chae, J. Lee, C.H. Lee, *J. Membr. Sci.* 483 (2015) 128-135.
31. A.K. Ghosh, V. Ramachandhran, M.S. Hanra, B.M. Misra, *J. Polym. Mater.* 15 (1998) 279.
32. C. Boo, M. Elimelech, S. Hong, *J. Membr. Sci.*, 444 (2013) 148-156.
33. J. Herron, US Patent 7, 445, 712 (2008).

Received: 20-12-2019

Accepted: 28-01-2020